https://doi.org/10.5194/wes-2026-177
Preprint. Discussion started: 3 November 2026
© Author(s) 2026. CC BY 4.0 License.



eawe european academy of wind energy
Open Access WIND ENERGY SCIENCE DISCUSSIONS

Development of a free online database related to a one-year experimental campaign for wind turbine noise

Gwenaël Guillaume[1], David Ecotière[1], Benoit Gauvreau[2], Fabrice Junker[3], Isabelle Schmich-Yamane[4], and Albert Alarcon[4]

[1]Cerema, Univ. Gustave Eiffel, UMRAE - 11 rue Jean Mentelin, F-67035 Strasbourg, France
[2]Univ. Gustave Eiffel, Cerema, UMRAE - Campus de Nantes - Route de Bouaye - CS4, Bouguenais Cedex, F-44344 Nantes, France
[3]EDF-Renewables - 100 Esplanade du Général de Gaulle, F-92932 Paris La Défense, France
[4]EDF-DTG - 134 Chemin de l'Étang, F-38950 Saint-Martin-le-Vinoux, France

Correspondence: Gwenaël Guillaume (gwenael.guillaume@cerema.fr), David Ecotière (david.ecotiere@cerema.fr), and Benoit Gauvreau (benoit.gauvreau@univ-eiffel.fr)

Abstract. The PIBE project represents the first collaborative research project in France specifically focused on wind turbine noise variability. A primary objective of the project was to assess in situ the experimental variability of acoustic indicators and influencing environmental parameters, and to compare these observations with the variability predicted by sound emission and propagation models. To achieve this goal, a comprehensive one-year measurement campaign was carried out over 410 consecutive days around a wind farm comprising eight turbines (80 m hub height, 90 m rotor diameter). Acoustic recordings were made using five class 1 sound level meters located at distances ranging from 325 to 1400 meters from the wind farm, continuously recording third-octave band spectra as well as A- and Z-weighted equivalent sound levels (L_{eq}), and statistical noise levels (L_{10}, L_{50}, and L_{90}). Simultaneously, several meteorological parameters were collected, in particular by using three 3D ultrasonic anemometers and a wind lidar system monitored meteorological conditions, including wind and temperature vertical profiles, which significantly influence sound propagation. Additional information was collected about extraneous noise (train, aircrafts, wind noise) that could contaminate measured wind farm noise. All collected data were post-processed and stored in a scalable database system optimized for fast querying access. To facilitate data exploration and analysis, a web application was developed, providing interactive and free access to the database with specific query, processing and visualization tools for end users (scientists, engineers, stakeholders, etc.).

1 Introduction

The PIBE project (Predicting the Impact of Noise from Wind Turbines) has adopted a multidisciplinary and comprehensive approach to understanding and studying solutions for mitigating wind turbine noise (Ecotière et al., 2024). This endeavor encompasses the entire noise generation and propagation chain, from detailed studies of aerodynamic noise sources on turbine blades (Raus et al., 2022; Cotté et al., 2024) to advanced modelling of noise estimation through the atmosphere toward local residents (Kayser et al., 2023b; Kayser, 2023). Given the complex interactions between all environmental factors influencing

https://doi.org/10.5194/wes-2026-177
Preprint. Discussion started: 3 November 2026
© Author(s) 2026. CC BY 4.0 License.



eawe european academy of wind energy
Open Access WIND ENERGY SCIENCE DISCUSSIONS

noise emission and propagation, extensive experimental validation is essential to improve the accuracy and reliability of noise prediction models.

To this end, the project partners have undertaken a one-year experimental campaign spanning over more than a year on a representative French wind farm site. This campaign involved simultaneous deployment of a wide array of acoustic and meteorological sensors, enabling comprehensive monitoring of wind turbine noise and its interaction with local atmospheric conditions. This rich dataset obtained through these efforts underwent post-processing to create a synchronized database combining acoustic indicators and meteorological measurements. This database serves as a valuable resource to quantify uncertainties related to the variability of the physical processes governing noise generation and propagation (Bianchetti et al., 2023; Kayser et al., 2023a). Ultimately, the insights gained from this work aim to support more reliable assessment of noise pollution risks and inform strategies to optimize both the environmental impact and energy efficiency of wind farms.

The structure of this article is as follows. Section 2 details the experimental protocol and instrumentation set-up during the one-year campaign. Section 3 presents the data post-processing workflow, including quality control and extraneous noise event detection. Section 4 introduces the open access online data mining tool developed to facilitate data exploration and analysis for end users (scientist, engineers, stakeholders, etc.). Section 5 presents some examples of analyses of the influence of wind conditions on the sound levels measured by each acoustic sensor, defining the upwind, downwind, and crosswind conditions for each acoustic sensor in relation to its location relative to the wind turbine axis. Finally, conclusions and perspectives are drawn in Section 6.

2 Experimental protocol and instrumentation

2.1 Experimental site

The wind farm is located in the centre of France and shares characteristics common to many wind farms in France. As illustrated on the map in Figure 1, it comprises eight wind turbines with hub heights of 80 m and blade lengths of 45 m, each capable of generating 3 MW of nominal electrical power. The site has a flat topography and a relatively low background noise environment with few sources of extraneous noise. It features evenly alternating wind regimes in the north-south direction, enabling the study of upwind and downwind propagation conditions compared to the line of wind turbines.

2.2 Measuring equipment

The experimental campaign was based on the deployment of multiple measurement devices over the wind farm site, as illustrated on the map in Figure 1 and pictures in Figure 2, that recorded timestamped data concerning both acoustic indicators and meteorological variables.

Regarding acoustic measurements, five class 1 sound level meters (SLM Acoem DUO model) designated by A1 to A5 on Figure 1 were installed on either side and at different distances from the line of wind turbines (A1 at 325 m, A2 at 650 m, A3 at 1250 m, A4 at 1000 m and A5 at 1400 m). The sound level meters (Figure 2(e)) recorded the evolution over time of continuous

https://doi.org/10.5194/wes-2026-177
Preprint. Discussion started: 3 November 2026
© Author(s) 2026. CC BY 4.0 License.

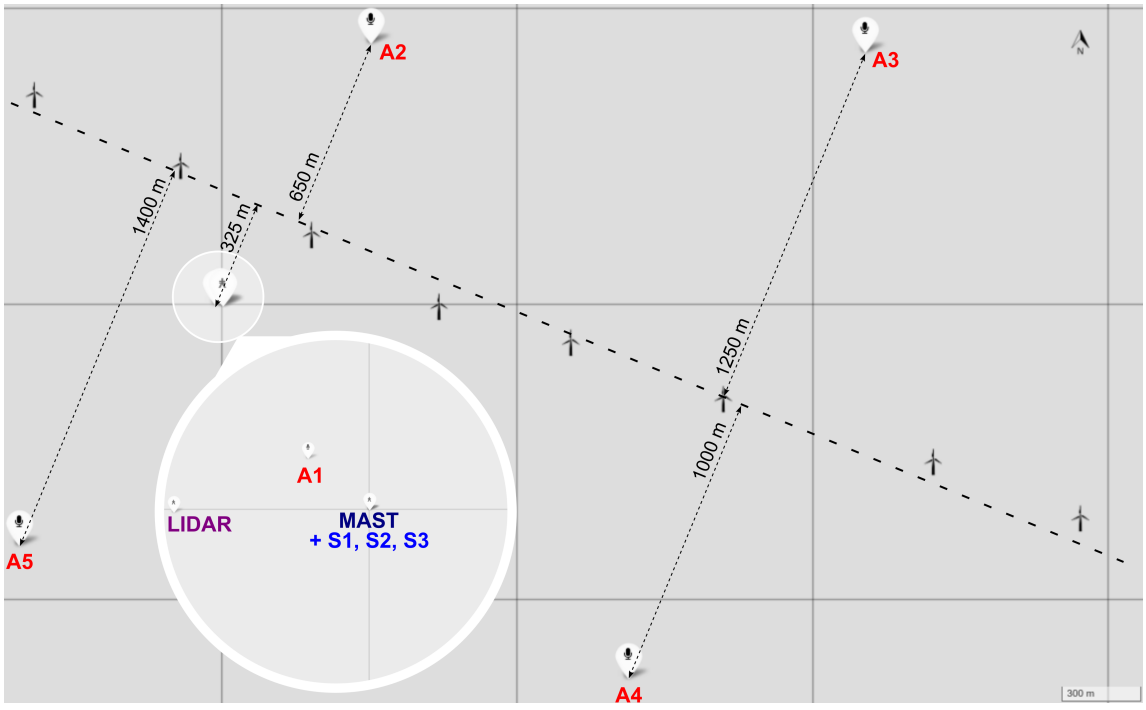


Figure 1. Mapping of the wind turbine farm and sensors deployed on site for the one-year experimental campaign. Note that the LIDAR and A1 devices within the zoomed-in area are located at the base of the mast.

equivalent sound pressure levels L_{eq} and fractile indicators L_{A10}, L_{A50} and L_{A90}, over integration periods of 100 ms, by third-octave bands and global values $L_{\text{Aeq},T}$ and $L_{\text{Zeq},T}$, in the form of daily spreadsheets. Additionally, as mentioned in Table 1, audio recordings in `wav` format were automated at 2-minute intervals every 10 minutes. This sampling scheme represents a trade-off between achieving sufficient temporal resolution to capture acoustic variability and limiting data storage requirements. It also ensures the ability to replay selected recordings for detailed post-processing without generating an excessive volume of data. The one-year acoustic measurements cover the period from January 28$^{\text{th}}$ 2020 (except A1: June 26$^{\text{th}}$ 2020) to March 31$^{\text{th}}$ 2021.

Table 1. Acoustic recordings by sound level meters (Acoem DUO model) deployed on-site for the one-year experimental campaign.

Variable	**Height (m)**	**Frequencies/sample rate (Hz)**
Continous equivalent A-weighted sound pressure level L_{Aeq}	1.5 (except A2 at 2.6m)	$f_{1/3\,oct.} \in [6.3; 20k]$ + global A & Z
Fractile indicators L_{A10}, L_{A50} and L_{A90}		
Audio recordings 2 min each 10 min		48k (24 bits)

https://doi.org/10.5194/wes-2026-177
Preprint. Discussion started: 3 November 2026
© Author(s) 2026. CC BY 4.0 License.



Figure 2. Measurement devices of the experimental campaign: (a) meteorological mast overview, (b) anemometers (3D ultrasonic anemometer in the foreground and three cup anemometer below), (c) temperature and relative humidity (THR) sensor, (d) wind lidar located close to the base of the mast (see Figure 1) and (e) sound level meter (SLM).

The presence of noise not originating from wind turbines, hereafter referred to as extraneous noise, could bias the analysis of the effect of meteorological conditions on acoustic measurements related to specific wind turbine noise. Thus, three strategies have been implemented to detect the presence of extraneous noise: audio recordings that have been automated with an additional sound recorder (Wildlife Acoustics Song Meter SM3) located near a railway track passing close to the site (at a distance of approximately 1.3 km of the nearest sound level meter A2, see Figure 1), manual inventory of aircraft overflights using the FlightRadar application, and estimation of the noise induced by wind on the microphones thanks to anemometers located

https://doi.org/10.5194/wes-2026-177
Preprint. Discussion started: 3 November 2026
© Author(s) 2026. CC BY 4.0 License.



eawe european academy of wind energy
Open Access WIND ENERGY SCIENCE DISCUSSIONS

near the five sound level meters at the same height as microphones (see Figure 1). These meteorological data were recorded in one-minute time slots.

Concerning meteorological measurements, a mast permanently on site (see Figure 2(a)) was equipped with various sensors and data acquisition systems, including temperature and humidity sensors (Figure 2(c)), three-cup anemometers, and rain gauges, at multiple heights (Table 2). Ten-minute averaged data from the mast were provided in spreadsheet format by the wind farm operator between the January 1st 2020 and April 4th 2021. In addition, certain SCADA data from wind turbines – namely the wind speed and direction at the turbine hub, and the rotational speed (RPM) – was also provided by the wind farm operator for each wind turbine over the period from February 1st 2020 to April1st 2021, with a sampling interval of 10 minutes. Table 2 summarizes information for meteorological sensors installed on the mast, including their models, heights, and configuration values, as well as SCADA data recorded at the hub level of each turbine.

Table 2. Meteorological variables recorded by the various sensors at different heights installed on the mast and on each turbine nacelle, with a 10-minute time sampling.

Variable	Unit	Height (m)	Sensor	Support
Temperature	°C	6, 20, 60, 78	Vaisala HMP45D	Mast
Wind direction	° rel. N	70, 80	Thies First Class	
Wind speed	$m.s^{-1}$	35, 75, 80		
Relative humidity	%	6, 20, 60, 78	Vaisala DTR503A	
Rainfall	mm	6	Vaisala DRD11A	
Atmospheric pressure	mbar	6	Setra M276	
Wind direction	° rel. N	80	–	Each turbine
Wind speed	$m.s^{-1}$			
RPM	$tr.min^{-1}$			

As part of this one-year experimental campaign, three 3D ultrasonic anemometers (Young 81000V) were mounted on the permanent meteorological mast (Figure 2(b)), from May 27th 2020 to May 26th 2021, at three heights: 10 m, 50 m and 80 m. These sensors, not mentioned in Table 2 because their measurements have undergone specific post-processing (see section 3.1), measure the Cartesian horizontal and vertical components U, V and W of the wind speed and virtual temperature T_v at 20 kHz sampling rate. A wind lidar (ZephIR ZX 300) was also installed at the foot of the meteorological mast, as illustrated at Figure 2(d), which measured, in particular, wind speeds and directions up to a height of around 200 m. The lidar provided time-stamped measurements in UTC format from June 23rd 2020 to March 3th 2021, with a variable sampling rate of around 15 s, in daily spreadsheets consisting of variables such as atmospheric pressure, temperature and relative humidity at 1 m height, rain and fog indicators (the fog indicator is the proportion of the period during which the Lidar measurement is invalid due to

https://doi.org/10.5194/wes-2026-177
Preprint. Discussion started: 3 November 2026
© Author(s) 2026. CC BY 4.0 License.



eawe european academy of wind energy
Open Access WIND ENERGY SCIENCE DISCUSSIONS

fog), horizontal and vertical wind speeds and directions at various heights from 10 m to 184 m high. All these information is summarized in Table 3.

Table 3. Meteorological variables provided by the wind lidar (ZephIR ZX 300) with a sampling time of approximately 15 s.

Variable	Unit	Height (m)
Atmospheric pressure	mbar	1
Temperature	°C	
Relative humidity	%	
Rainfall	mm	
Fog indicator	%	
Horizontal wind speed Vertical wind speed	$m.s^{-1}$	10, 20, 39, 40, 55, 70, 85, 100, 115, 130, 145, 165, 185
Wind direction	° rel. N	

3 Data post-processing

3.1 Acoustic and meteorological data

Raw acoustic and meteorological data from the one-year experimental campaign were post-processed to create a consolidated database, with a common UTC timestamping.

The acoustical data (see Table 1) were reprocessed to produce timestamped indicators based on 3 common UTC intervals of 100 ms, 1 m and 10 min.

The post-processing of SCADA data and meteorological data issued from the sensors permanently installed on the mast (see Table 2) consisted in extracting useful information from the meteorological data supplied by all the sensors deployed as part of the experimental campaign. This data is only available with a time representativeness of 10 min. Similarly, the raw data provided by the wind lidar with a variable timestamping of around 15 s have been post-processed to calculate the meteorological variables over time intervals of 1 min and 10 min. Data from the three 3D ultrasonic anemometers with a sampling rate of 20 Hz have been entirely post-processed to calculate the meteorological variables listed in Table 4 over periods of 1 min and 10 min. Monin Obukhov length, friction velocity, sensible heat flux, turbulent kinetic energy and aerodynamic roughness height are derived from 3D wind speeds from sonic anemometer and using the eddy-covariance theory (Foken, 2008). Vertical gradient of wind speed and temperature are derived from the Monin Obukhov theory. In table 4, data completeness corresponds to the percentage of valid data for the whole period.

https://doi.org/10.5194/wes-2026-177
Preprint. Discussion started: 3 November 2026
© Author(s) 2026. CC BY 4.0 License.



eawe european academy of wind energy
Open Access WIND ENERGY SCIENCE DISCUSSIONS

Table 4. Meteorological variables issued from the post-processing of the 3D ultrasonic anemometers (Young 81000V model) measurements for the one-year experimental campaign.

Variable	Unit
Mean and standard deviation of wind speed	$m.s^{-1}$
Mean and standard deviation of virtual temperature	°C
Mean and standard deviation of wind direction	° rel. N
Turbulent kinetic energy	$m^2.s^{-2}$
Friction velocity	$m.s^{-2}$
Sensible heat flux	J
Monin–Obukhov length	m
Aerodynamic roughness height	m
Temperature gradient	$°.m^{-1}$
Wind speed vertical gradient	s^{-1}
Sound speed vertical gradient	s^{-1}
Data completeness	%

3.2 Extraneous noise event detection

The data collected to indicate the possible presence of extraneous noise events such as trains passages, aircraft overflights and wind induced noise at microphones were also post-processed in order to use this information a posteriori for data analysis by filtering the corresponding timestamps in the dataset.

To detect passing trains, audio recordings from the sound recorder located near the high-speed rail line – at approximately 1.3 km from the nearest acoustic sensor (A2, see Figure 1) – were automatically triggered using an empirical threshold detection. Train passages were recorded in spreadsheets using UTC timestamps at 1-minute and 10-minute intervals. Each entry was marked with a 1 when a train passed, 0 otherwise, and 'NA' for periods without valid data (equipment malfunction). A rough estimation indicates that only a very small proportion of the data would be likely to be affected by railway traffic noise (see Table 5).

Aircraft overflights were manually referenced to the minute between February 2020 and February 2021 using the FlightRadar application, which provides aircraft position data in real time or retrospectively. This process involved recording, in monthly spreadsheets, the UTC timestamps corresponding to aircraft entering and leaving a 25 km by 25 km area centered on the wind farm. As with train passages, an *aircraft* column was appended to the previous time-stamped spreadsheet which takes

https://doi.org/10.5194/wes-2026-177
Preprint. Discussion started: 3 November 2026
© Author(s) 2026. CC BY 4.0 License.



eawe european academy of wind energy
Open Access WIND ENERGY SCIENCE DISCUSSIONS

the value 1 when an aircraft overflied the study zone, 0 otherwise, and NA for periods of no valid data. As summarized in Table 5, a higher occurence of aircraft overflights is estimated in comparison to train passages, meaning that a more substantial share of acoustic data could potentially be polluted, especially since the inventory of aircraft overflights was not drawn up over the entire experimental campaign. The noise spectra associated with wind turbine noise also exhibit similarities to aircraft noise (low-frequency content). Nonetheless, the presence of an aircraft over the study zone does not necessarily imply that the recordings made by acoustics sensors are corrupted.

Table 5. Percentage of occurrences of extraneous noise events (1 min data) associated with passing trains or aircraft (1: passage detected, 0: no passage detected, NA: no valid data).

Source	Percentage of occurrence (%)		
	Undefined	0	1
Train	45.2	54.3	0.5
Aircraft	11.2	71.0	17.8

The wind-induced bias on the sound levels measured by acoustic sensors A1 to A5, as well as the uncertainty associated with its estimation, was assessed using the methodology described in (Ecotière, 2018). The validity of the bias estimation model and its associated uncertainty was first controlled at the one-minute scale by verifying the availability and validity of both the measured sound levels and wind speeds. Afterwards, the influence of wind induced noise at microphone is estimated for each time slot, by checking that the measured A-weighted global sound pressure does not exceed a critical value that depends on wind speed at microphone level and on sound level (Ecotière (2018); NF S31-120).

4 Online data mining tool

A structured data storage system has been implemented and coupled with a web-based graphical interface designed to facilitate the exploration, querying, and retrieval of validated post-processed experimental data. This architecture is illustrated in Figure 3, which highlights the secure interaction between the data repository and the user interface.

The experimental data management system is built upon ElasticSearch, an open access platform designed for efficient indexing and rapid querying of large datasets. This technology was chosen for its scalability and flexibility in processing various data streams, as well as for its powerful analytical capabilities, which are essential for efficient long-term data storage, retrieval, and analysis. The ElasticSearch database has thus been set up to store the post-processed measurement data collected during the experimental campaign. A container-based deployment strategy, implemented with Docker, was adopted to encapsulate the database system and its environment, ensuring consistency and reproducibility across different computing platforms. The database is deployed on a remote server using a containerized infrastructure managed with Docker and orchestrated via a *docker-compose.yml* configuration file, which ensures seamless setup of both the ElasticSearch and Kibana services. This configuration includes predefined environment variables, port mapping, data volumes for persistence, and network settings

https://doi.org/10.5194/wes-2026-177
Preprint. Discussion started: 3 November 2026
© Author(s) 2026. CC BY 4.0 License.

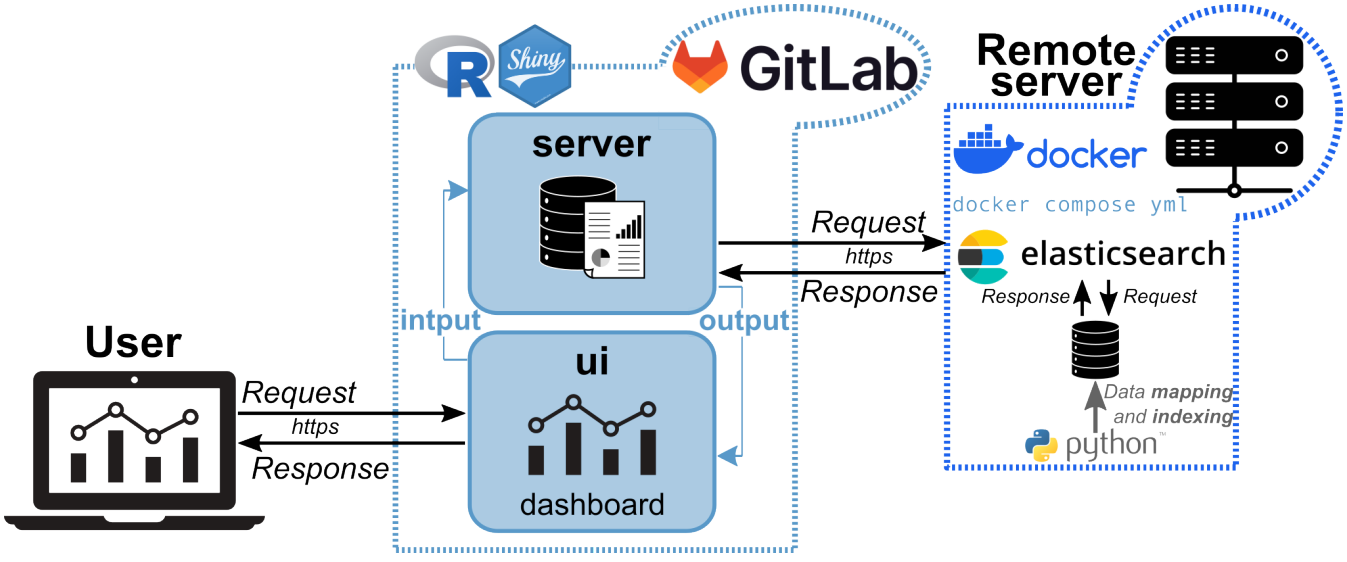


Figure 3. Scheme of the data mining application framework.

for internal communication between services. Once deployed, the database is filled using a dedicated Python script that automatically connects to the ElasticSearch instance, defines mappings, and indexes structured datasets. This script handles the integration of the post-processed experimental data, including acoustic energy and statistical indicators (Table 1), extraneous noise detection events, and meteorological variables (Tables 2, 3 and 4). The ingestion logic also includes metadata tagging to facilitate efficient retrieval, aggregation, and visualization of the stored data.

To facilitate access to this data repository, a User-oriented web application has been developed using the Shiny framework, providing researchers and analysts with secure and interactive access to the underlying database. Through this application, users can easily explore the indexed data, perform custom queries based on specific parameters, download selected dataset, and visualize trends and patterns via interactive plots. The application is fully developed in the R programming language and its source code is managed under version control using GitLab. A continuous integration and deployment (CI/CD) pipeline has been implemented to automate application updates: each change pushed to the development branch (*dev*) triggers an automatic deployment to a private web application hosting environment shinyapps.io, allowing for testing and validation. Once developments on the *dev* branch are approved and merged into the main branch (*main*), a second CI/CD pipeline ensures the updated application is automatically deployed to the public shinyapps.io environment. This dual-pipeline strategy guarantees that end-users always interact with a stable and functional version of the application, while maintaining a flexible workflow for fixing bugs, improving the interface, and expanding functionality. This free interface is organized into three main tabs:

- the first tab, titled *PIBE project*, presents contextual information about the project and one-year experimental campaign. It includes an interactive map showing the location of the wind turbines and the geographical distribution of the deployed sensors with a dynamic table that describes each sensor's type, model, measured variables and height. This section aims

https://doi.org/10.5194/wes-2026-177
Preprint. Discussion started: 3 November 2026
© Author(s) 2026. CC BY 4.0 License.



to provide users with an overview of the sensor network used for in situ monitoring and the overall objectives of the PIBE initiative;

- the second tab, called *Data download*, is dedicated to defining and executing data extraction queries. Users can specify time intervals (start and end dates), select the time resolution (1-minute or 10-minute averages), and choose which acoustic and/or meteorological sensors and variables to include. Additional filtering options are available, such as excluding data corresponding to train or aircraft passings, or applying meteorological thresholds to refine the selection. A map displays the selected sensors in real-time based on user input to help select appropriate sensors;

- the third tab, named *Visualization*, provides a suite of interactive data exploration tools. Users can load the dataset previously extracted in the *Data download* tab and visualize it through time series or scatter plots, with customizable options for selecting variables on the x- and y-axes. These plots allow for the identification of temporal trends, correlations between variables, and the detection of anomalies or specific events. Additionally, a data table is integrated to facilitate direct control of the loaded data set.

5 Example of application: data extraction for the analysis of wind-related propagation conditions and wind turbine noise data

The following classification of wind-dependent sound propagation conditions is based on the geometric orientation of the line of wind turbines (see Figure 1). The main axis of the wind farm is inferred from the spatial arrangement of the turbines using a linear regression of their coordinates, that provides a reliable estimate of the longitudinal orientation of the wind farm. The resulting axis vector is converted into an azimuth bearing with respect to "true" North (i.e., 120.9°). This bearing defines the conditions of upwind and downwind for the acoustic sensors in relation to the wind farm and constitutes the reference from which wind directions relative to acoustic sensors are evaluated and classified into three regimes:

- *upwind*, when the wind flow is perpendicular to the wind farm and oriented from the wind farm toward the acoustic sensor,

- *downwind*, when the wind flow is perpendicular to the wind farm and oriented from the acoustic sensor toward the wind farm,

- *crosswind*, when the incident wind is collinear to the turbine array–receiver line.

Figure 4 shows the resulting wind-exposure configuration, with the acoustic sensor positions and the wind directions corresponding to the upwind, downwind and crosswind classes materialized by arrows at each sensor.

Table 6 summarises, for each acoustic sensor, the nominal wind directions associated with upwind, downwind and crosswind regimes, together with the corresponding statistical descriptors of the A-weighted sound pressure level L_{Aeq} recomposed in samples of 10-minute duration. Wind direction classes are defined using the SCADA measurements from the eight turbines of the wind farm: each class is assigned only when the wind directions for all wind turbines are within a tolerance of $\pm 15°$ around

https://doi.org/10.5194/wes-2026-177
Preprint. Discussion started: 3 November 2026
© Author(s) 2026. CC BY 4.0 License.

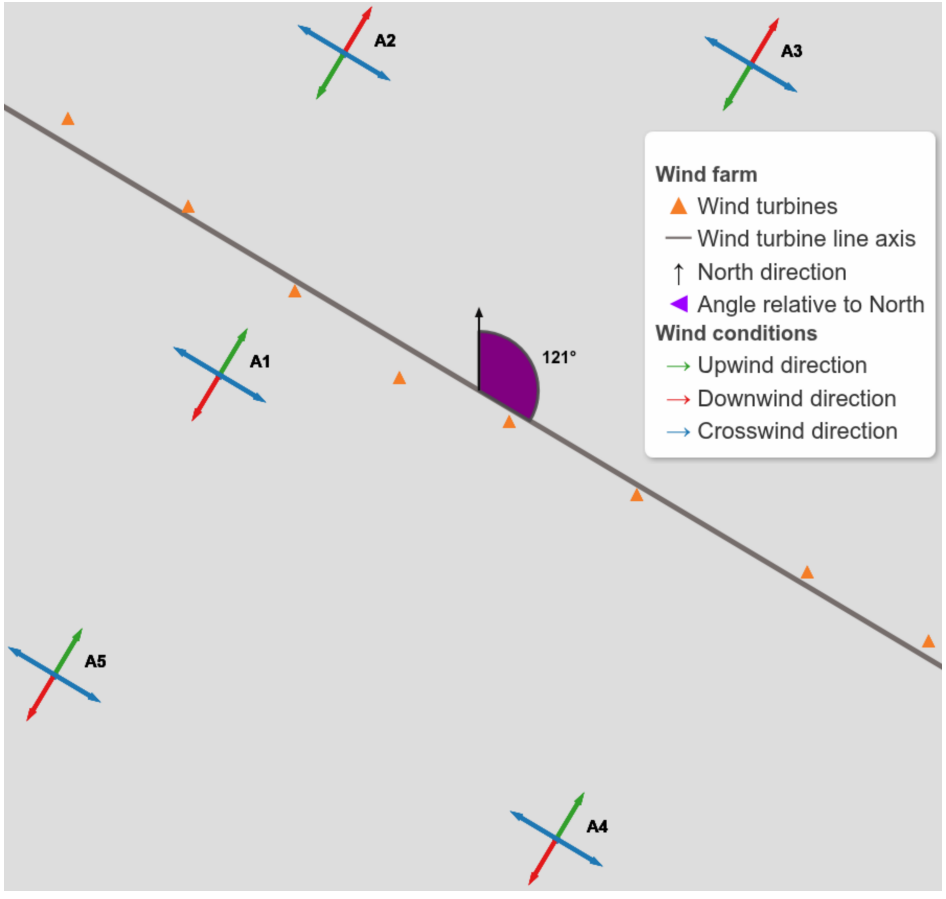


Figure 4. Mapping of the wind conditions at each acoustic sensor. The direction of the arrows on each acoustic sensor indicates the wind direction at the sensor location for each wind class.

the nominal direction defining that class, and the wind speed at hub height is 3 m.s^{-1} or higher. For each propagation condition, the table reports the minimum, arithmetic mean, standard deviation and maximum of L_{Aeq} after removing time periods likely to be affected by aircraft or train passages (other factors, such as rainfall, are not taken into account in the data filtering).

Table 6 also shows that north-easterly winds – which correspond to upwind conditions for the sensors located southwest of the turbine row (A1, A4 and A5) and to downwind conditions for those located northeast of the row (A2 and A3) – are by far the most frequently encountered. This regime occurs nearly twice as long as the two other wind classes, consistent with the prevailing wind climatology of the region where the wind farm is located. As expected, the mean and standard deviation of L_{Aeq} for the triplet A1, A4, and A5 are slightly higher by several dBA under upwind conditions than under downwind conditions. Conversely, the opposite behaviour appears for the pair of sensors A2 and A3, for which the sound levels for downwind conditions are higher than those for upwind conditions. This can also be observed in the figure 5 that shows the distribution of the L_{Aeq} by wind regime for each acoustic sensor. For A1, which is the sensor closest to the wind turbine axis,

https://doi.org/10.5194/wes-2026-177
Preprint. Discussion started: 3 November 2026
© Author(s) 2026. CC BY 4.0 License.



eawe european academy of wind energy
Open Access WIND ENERGY SCIENCE DISCUSSIONS

Table 6. Angles defining each wind class, durations of occurrence with valid acoustic measurements, and statistics of the L_{Aeq} indicator for each acoustic sensor. A tolerance of $\pm 15°$ around the nominal values of wind class angles is used to determine the duration of occurrence and statistical variables, and periods during which the wind speed is less than 3 m.s^{-1} are not considered.

Sensor	Wind class	Angle (°)	Hours (h)	$L_{\text{Aeq,min}}$	$L_{\text{Aeq,avg}}$	$L_{\text{Aeq,std}}$	$L_{\text{Aeq,max}}$
A1	Upwind	211	88.0	26.4	54.2	6.2	69.7
	Downwind	31	37.5	27.2	46.7	5.2	57.9
	Crosswind	(121, 301)	29.2	25.6	54.3	9.4	74.0
A2	Upwind	31	37.7	23.1	44.2	8.3	63.3
	Downwind	211	88.5	26.9	57.2	8.3	77.5
	Crosswind	(121, 301)	31.3	24.2	61.9	10.0	82.3
A3	Upwind	31	37.5	22.1	35.7	5.2	48.9
	Downwind	211	87.7	26.7	46.8	6.1	61.1
	Crosswind	(121, 301)	31.0	24.5	39.1	4.2	49.5
A4	Upwind	211	88.2	25.0	46.7	10.9	70.7
	Downwind	31	37.7	23.9	45.0	9.0	63.9
	Crosswind	(121, 301)	31.3	24.5	61.8	8.4	78.9
A5	Upwind	211	88.2	22.3	45.8	8.4	67.0
	Downwind	31	37.7	21.0	42.7	6.3	57.8
	Crosswind	(121, 301)	31.3	21.7	46.6	7.3	63.3

the L_{Aeq} varies almost linearly with wind speed. It is noteworthy that the spreading of L_{Aeq} in this wind speed span is much greater the further away from the wind farm, reaching its maximum at sensor A5, which is the furthest from the turbine farm axis and consistent with our knowledge of physical phenomena related to long range sound propagation.

To assess whether the differences observed in Table 6 are statistically meaningful, pairwise Welch t-tests are performed between the upwind, downwind and crosswind data subsets for each acoustic sensor. The resulting p-values are reported in Table 7, where significance levels are indicated by asterisks.

The statistical analysis generally confirms the trends already observed in Table 6. For sensors A1 and A2, highly significant differences are found between upwind and downwind conditions ($p < 0.001$), whereas no significant difference appears between either of these conditions and crosswind conditions. These results support the interpretation that the dominant contrast at these locations is associated with the reversal of wind direction relative to the wind farm. Sensor A3 exhibits the clearest dependence on wind direction, with all pairwise comparisons being statistically significant ($p < 0.001$). In agreement with the mean values reported in Table 6, the average A-weighted equivalent sound level $L_{\text{Aeq,avg}}$ increases from upwind to crosswind and reaches its highest values under downwind conditions. A different behaviour is observed for sensor A4 since no statistically significant difference is detected between upwind and downwind conditions, despite a small difference in $L_{\text{Aeq,avg}}$, whereas the

https://doi.org/10.5194/wes-2026-177
Preprint. Discussion started: 3 November 2026
© Author(s) 2026. CC BY 4.0 License.

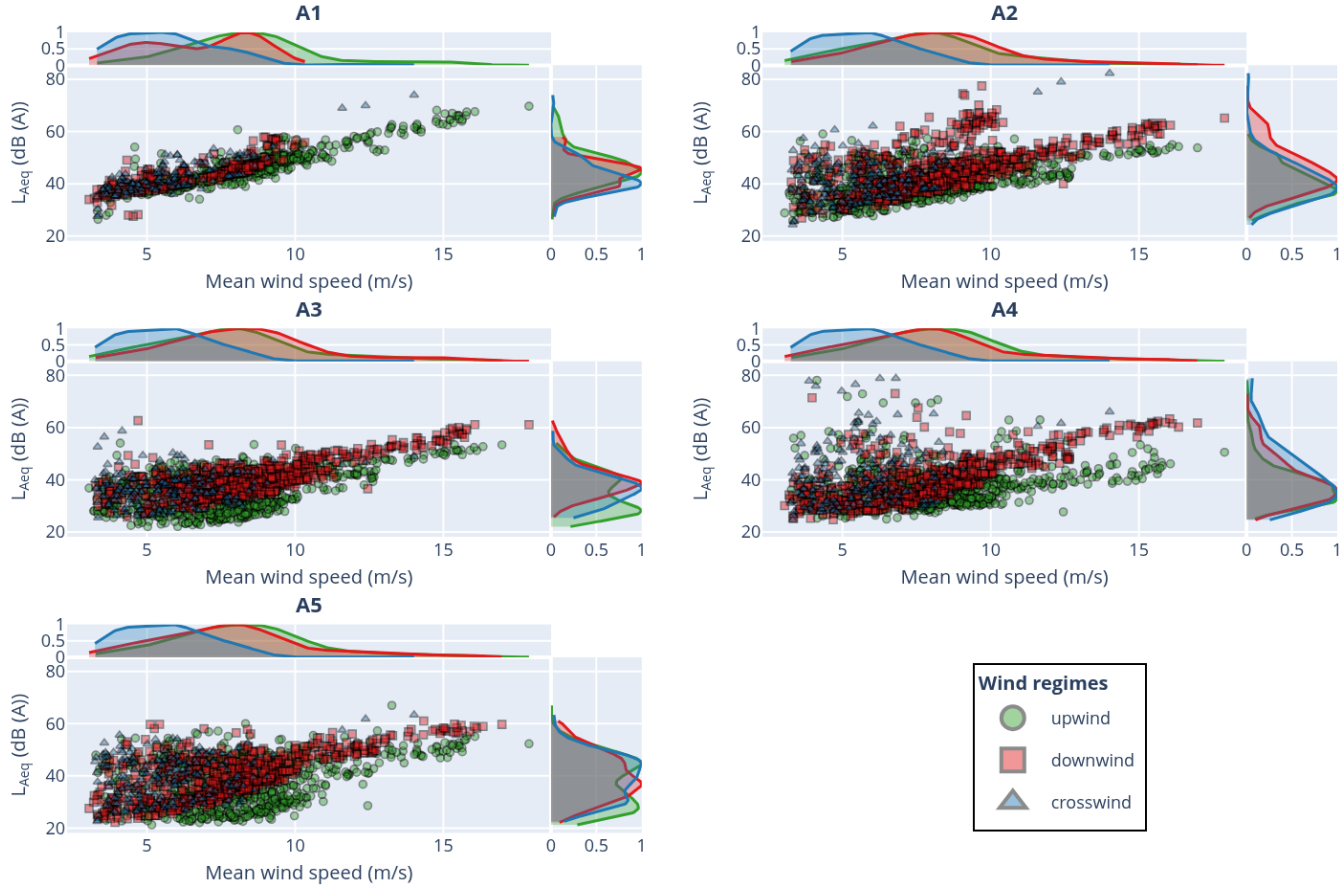


Figure 5. A-weighted continuous equivalent sound pressure levels L_{Aeq} for upwind, downwind and crosswind meteorological conditions (10 min data). Periods are selected when all wind directions and speeds at the hub level of the wind turbines are respectively within $\pm 15°$ of the regime angle and $\geqslant 3$ m.s^{-1}.

crosswind regime differs significantly from both of the other classes. Finally, none of the comparisons involving sensor A5 reaches the 5% significance level. Although the $L_{\mathrm{Aeq,avg}}$ values differ by a few decibels between wind classes, these differences remain small compared with the observed variability of the measurements and therefore cannot be considered statistically significant. Overall, the results indicate that the influence of wind direction on L_{Aeq} is most pronounced at sensors A1, A2 and particularly A3, while it becomes progressively less distinct at the more distant sensors A4 and A5.

https://doi.org/10.5194/wes-2026-177
Preprint. Discussion started: 3 November 2026
© Author(s) 2026. CC BY 4.0 License.



eawe european academy of wind energy
Open Access WIND ENERGY SCIENCE DISCUSSIONS

Table 7. Welch t-tests comparing L_{Aeq} distributions between wind classes. Significance levels are denoted by * for $p < 0.05$ and *** for $p < 0.001$.

Sensor	Upwind vs Downwind	Upwind vs Crosswind	Downwind vs Crosswind
A1	$< 0.001^{***}$	0.974	0.159
A2	$< 0.001^{***}$	0.136	0.322
A3	$< 0.001^{***}$	$< 0.001^{***}$	$< 0.001^{***}$
A4	0.572	0.027^{*}	0.026^{*}
A5	0.075	0.650	0.074

6 Conclusion

This paper presented the comprehensive experimental framework established as part of the PIBE project to study the variability of wind turbine noise both coming from the generation and propagation phenomena. The one-year measurement campaign has provided an extensive dataset of synchronized acoustic and meteorological parameters that capture the complex variability of atmospheric conditions that influence both emission and propagation of wind turbine noise.

The thorough post-processing procedures applied to measurements ensure its reliability and robustness for subsequent modelling and analysis. The development of a free interactive online data mining tool further enhances accessibility, enabling researchers to explore, filter, and analyse the data efficiently.

Beyond constituting a valuable resource for the scientific community, the dataset also provides a solid experimental basis for advancing noise modelling approaches. Future work will exploit these measurements to refine noise prediction models, better characterise meteorological influences on both emission and propagation, and improve the quantification of uncertainties associated with wind turbine noise predictions or assessment. These advancements will contribute to a better assessment of wind turbine noise impact, and support the design of quiet and sustainable wind energy projects.

Data availability. The post-processed dataset can be consulted via the User-oriented web application and can also be downloaded on an open repository (https://doi.org/10.5281/zenodo.15721844, Guillaume et al., 2025).

Video supplement. A video presentation of the PIBE project and the one-year experimental campaign is available on this link: https://www.youtube.com/watch?v=X_VGP26v6Ew.

Author contributions. The preparation of the article was led by GG, with contributions from all the authors. The long-term experimental campaign was coordinated by BG and DE, in the framework of the PIBE project (leader DE). We gratefully acknowledge EDF power

https://doi.org/10.5194/wes-2026-177
Preprint. Discussion started: 3 November 2026
© Author(s) 2026. CC BY 4.0 License.



eawe european academy of wind energy
Open Access WIND ENERGY SCIENCE DISCUSSIONS

240 solutions for facilitating access to the experimental wind farm site and enabling the provision of SCADA data by FJ. The acoustic data were coordinated and processed by AA and ISY. The meteorological data and data relating to the detection of noise events were processed by GG. The software infrastructure (Docker website, Elasticsearch database, Shiny framework and CI/CD pipeline) was developed and implemented by GG.

Competing interests. The contact author has declared that neither of the authors has any competing interests.

245 *Acknowledgements.* This research is funded by the French National Agency for Research (PIBE project) within the convention N°ANR-18-CE04-0011. The authors would also like to thank the contributors to this work: the technicians, engineers, and researchers, and in particular Hubert Lefèvre (Cerema) and Benjamin Cotté (UMR 9219, CNRS-ENSTA Paris-EDF-CEA).

https://doi.org/10.5194/wes-2026-177
Preprint. Discussion started: 3 November 2026
© Author(s) 2026. CC BY 4.0 License.



eawe european academy of wind energy
Open Access WIND ENERGY SCIENCE DISCUSSIONS

References

Bianchetti, S., Kayser, B., Guillaume, G., Gauvreau, B., Notarantonio, A., Junker, F., and Ecotière, D.: Variability and uncertainty of wind farm noise: A comparison between numerical predictions and in-situ measurements, in: Proceedings of Forum Acusticum, Torino, Italy, https://doi.org/10.61782/fa.2023.1063, 2023.

Cotté, B., Sicard, L., Raus, D., Monchaux, R., Jondeau, E., Souchotte, P., and Roger, M.: Experimental characterization of stall noise on a pitching airfoil in an anechoic wind tunnel, in: Proceedings of Inter-Noise, Nantes, France, https://doi.org/10.3397/IN_2024_4183, 2024.

Docker: Docker website, https://www.docker.com/.

Ecotière, D.: A semi analytical model to estimate the uncertainties of wind-induced noise in a screened microphone, in: Proceedings of Inter-Noise, Chicago, USA, 2018.

Ecotière, D., Gauvreau, B., Cotté, B., Roger, M., Schmich-Yamane, I., and Junker, F.: Predicting the impact of wind turbine noise: general overview and results of the PIBE project, in: Proceedings of Inter-Noise, Nantes, France, https://doi.org/https://doi.org/10.3397/IN_2024_4217, 2024.

ElasticSearch: ElasticSearch website, www.elastic.co/fr/elasticsearch/.

FlightRadar: FlightRadar website, www.flightradar24.com.

Foken, T.: Micro-meteorology, Springer-Verlag, Berlin, Heidelberg, ISBN 978-3-642-25440-6, https://doi.org/10.1007/978-3-642-25440-6, 2008.

Guillaume, G., Écotiere, D., and Gauvreau, B.: Acoustic and meteorological long-term measurement dataset from a wind farm monitoring campaign within the PIBE project, Zenodo, https://doi.org/10.5281/zenodo.15721844, 2025.

Kayser, B.: Open access of a wide-angle parabolic equation model for sound propagation in a moving atmosphere above an absorbing and rough ground, in: Proceedings of Forum Acusticum, Torino, Italy, https://doi.org/10.61782/fa.2023.0369, 2023.

Kayser, B., Bianchetti, S., Ecotière, D., and Gauvreau, B.: WindTUNE: a new tool for modelling wind farm noise uncertainties, in: Proceedings of the 10th International Conference on Wind Turbine Noise, Dublin, Ireland, 2023a.

Kayser, B., Mascarenhas, D., Cotté, B., Ecotière, D., and Gauvreau, B.: Validity of the effective sound speed approximation in parabolic equation models for wind turbine noise propagation, The Journal of the Acoustical Society of America, 153, 1846–1854, https://doi.org/10.1121/10.0017653, 2023b.

NF S31-120: Acoustics - Description and measurement of environmental noise - Soil and weather conditions influence, 2018.

PIBE: PIBE project website, https://www.anr-pibe.com/en.

Raus, D., Cotté, B., Monchaux, R., Jondeau, E., Souchotte, P., and Roger, M.: Experimental study of the dynamic stall noise on an oscillating airfoil, Journal of Sound and Vibration, 537, 117 144, https://doi.org/https://doi.org/10.1016/j.jsv.2022.117144, 2022.

Shiny: https://shiny.posit.co/.

User-oriented web application: Data mining application for the PIBE project's experimental campaign, https://cerema-med.shinyapps.io/pibe-app/.